Available online at www.sciencedirect.com
ScienceDirect
Journal of Organometallic Chemistry 692 (2007) 824–830
Journal of Organometallic Chemistry
www.elsevier.com/locate/jorganchem

Ortho-metallated ruthenium(III) complexes with some acid hydrazide based Schiff bases

Raji Raveendran, Samudranil Pal *

School of Chemistry, University of Hyderabad, Hyderabad 500 046, India

Received 16 September 2006; received in revised form 12 October 2006; accepted 12 October 2006
Available online 19 October 2006

Abstract

Ortho-metallated ruthenium(III) complexes with Schiff bases (H_2L) derived from one mole equivalent each of benzaldehyde and acid hydrazides are described. Reactions of H_2L with $[Ru(PPh_3)_3Cl_2]$ in presence of NEt_3 (1:1:2 mole ratio) under aerobic conditions in methanol provide the complexes having the general formula *trans*-$[Ru(L)(PPh_3)_2Cl]$ in 55–60% yields. The complexes have been characterized with the help of elemental analysis, magnetic susceptibility, electrochemical and various spectroscopic (infrared, electronic and EPR) measurements. The +3 oxidation state of the metal centre in these complexes is confirmed by their one-electron paramagnetic nature. Molecular structures of two representative complexes have been determined by X-ray crystallography. In each complex, the metal ion is in a distorted octahedral $CNOClP_2$ coordination sphere. The dianionic C,N,O-donor ligand (L^{2-}) together with the chloride form a CNOCl square-plane and the P-atoms of the two PPh_3 molecules occupy the two axial sites. The electronic spectra of the complexes in dichloromethane solutions display several absorptions due to ligand-to-metal charge transfer and ligand centred transitions. In dichloromethane solutions, the complexes display a ruthenium(III) → ruthenium(IV) oxidation in the potential range 0.35–0.98 V (vs. Ag/AgCl). All the complexes in frozen (110 K) dichloromethane–toluene (1:1) solutions display rhombic EPR spectra.

Keywords: Ruthenium(III); Schiff bases; Acid hydrazides; Cyclometallation; Crystal structures

1. Introduction

Organometallic complexes of ruthenium are essentially limited to its diamagnetic +2 oxidation state [1,2]. Only a few examples of authentic ruthenium(III)–C σ-bond containing species with carbonyl or non-carbonyl ligand systems are known [3–13]. Among the non-carbonylic systems cyclometallated species are very rare. The few examples known are with tridentate aromatic-C, azo- or imine-N and phenolate-O coordinating ligands [10–13]. These complexes are one-electron paramagnetic and EPR active. The X-ray crystal structure of one of these complexes with the C,N,O-donor azophenolate has been reported [10].

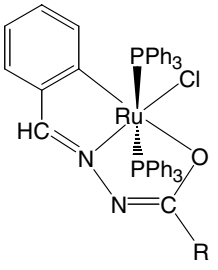

$[Ru(L^1)(PPh_3)_2Cl]$ (**1**) (R = CH_3)
$[Ru(L^2)(PPh_3)_2Cl]$ (**2**) (R = C_6H_5)
$[Ru(L^3)(PPh_3)_2Cl]$ (**3**) (R = 4-CH_3-C_6H_5)
$[Ru(L^4)(PPh_3)_2Cl]$ (**4**) (R = 4-OCH_3-C_6H_5)
$[Ru(L^5)(PPh_3)_2Cl]$ (**5**) (R = 4-Cl-C_6H_5)
$[Ru(L^6)(PPh_3)_2Cl]$ (**6**) (R = 4-NO_2-C_6H_5)

We have been working on the Schiff bases (H_2L) derived from acid hydrazides and aromatic aldehydes, which can act as monoanionic or bianionic tridentate aromatic-C, imine-N and amide-O donor ligands to provide cyclometallated complexes. Recently, we have reported some *ortho*-palladated species with H_2L [14,15]. These results prompted us to explore the possibility of using this Schiff

* Corresponding author. Tel.: +91 40 2313 4756; fax: +91 40 2301 2460.
E-mail address: spsc@uohyd.ernet.in (S. Pal).

0022-328X/$ - see front matter © 2006 Elsevier B.V. All rights reserved.
doi:10.1016/j.jorganchem.2006.10.026

base system for the synthesis of new *ortho*-metallated ruthenium species using the 16-electron starting material $[Ru(PPh_3)_3Cl_2]$. In this effort, we have isolated a series of paramagnetic ruthenium(III) organometallic complexes of C,N,O-coordinating L^{2-}. In the following account, we have described the synthesis, structure and physical properties of these complexes having the general molecular formula *trans*-$[Ru(L^n)(PPh_3)_2Cl]$ ($n = 1$–6).

2. Experimental

2.1. Materials

The Schiff bases H_2L^n ($n = 1$–6) were prepared in 60–80% yields by condensation reactions of 1 mole equiv. of benzaldehyde with 1 mol equiv. of the corresponding acid hydrazide in methanol. $[Ru(PPh_3)_3Cl_2]$ was prepared by following a reported procedure [16]. All other chemicals and solvents were of analytical grade available commercially and were used without further purification.

2.2. Physical measurements

Microanalytical (C, H, N) data were obtained with a Thermo Finnigon Flash EA1112 series elemental analyzer. Infrared spectra were collected by using KBr pellets on a Jasco-5300 FT-IR spectrophotometer. A Shimadzu 3101-PC UV/vis/NIR spectrophotometer was used to record the electronic spectra. EPR spectra were recorded on a Jeol JES-FA200 spectrometer. Magnetic susceptibilities were measured using a Sherwood Scientific balance. Diamagnetic corrections calculated from Pascal's constants [17] were used to obtain the molar paramagnetic susceptibilities. Solution electrical conductivities were measured with a Digisun DI-909 conductivity meter. A CH-Instruments model 620A electrochemical analyzer was used for cyclic voltammetric experiments with dichloromethane solutions of the complexes containing tetrabutylammonium perchlorate (TBAP) as the supporting electrolyte. The three electrode measurements were carried out at 298 K under dinitrogen atmosphere with a platinum disk working electrode, a platinum wire auxiliary electrode and an Ag/AgCl reference electrode. Under identical condition the Fc^+/Fc couple was observed at 0.65 V. The potentials reported in this work are uncorrected for junction contributions.

2.3. Synthesis of $[Ru(L^1)(PPh_3)_2Cl]$ (1)

Solid $[Ru(PPh_3)_3Cl_2]$ (300 mg, 0.31 mmol) was added to a methanol solution (30 ml) of H_2L^1 (50 mg, 0.31 mmol) and $N(C_2H_5)_3$ (0.09 ml, 65 mg, 0.65 mmol) and the mixture was heated under reflux for 2 h. On cooling to room temperature the complex was precipitated as a yellow solid. It was collected by filtration and washed with hexane. The solid was dissolved in dichloromethane–acetonitrile (1:6) mixture (7 ml). Hexane (4 ml) was added to this solution and left in air for slow evaporation. The crystalline complex separated in about 2 days was collected by filtration and dried in air. Yield, 150 mg (59%). A single crystal suitable for X-ray structure determination was collected from this material.

2.4. Synthesis of $[Ru(L^2)(PPh_3)_2Cl]$ (2)

Solid $[Ru(PPh_3)_3Cl_2]$ (300 mg, 0.31 mmol) was added to a methanol solution (35 ml) of H_2L^2 (70 mg, 0.31 mmol) and $N(C_2H_5)_3$ (0.09 ml, 65 mg, 0.65 mmol) and the mixture was stirred at room temperature for 2 h. The orange-red solid precipitated was collected by filtration, washed with hexane and finally dried in air. Yield, 165 mg (60%).

The other complexes (**3**–**6**) reported in this work were synthesized in 55–60% yields by following the same general procedure as described above for **2**. In powder form, complexes **3**–**5** are orange-red in colour as **2**, while complex **6** is dark-brown in colour. Among complexes **2**–**6**, single crystals of only **3** could be obtained by the same way as described for **1**.

2.5. X-ray crystallography

Unit cell parameters and the intensity data for **1** and **3** were obtained on a Bruker-Nonius SMART APEX CCD single crystal diffractometer, equipped with a graphite monochromator and a Mo Kα fine-focus sealed tube ($\lambda = 0.71073$ Å) operated at 2.0 kW. The detector was placed at a distance of 6.0 cm from the crystal and the data were collected at 298 K with a scan width of 0.3° in ω and an exposure time of 15 s/frame. The SMART software was used for data acquisition and the SAINT-PLUS software was

Table 1
Crystallographic data for *trans*-$[Ru(L^1)(PPh_3)_2Cl]$ (**1**) and *trans*-$[Ru(L^3)(PPh_3)_2Cl]$ (**3**)

Complex	**1**	**3**
Chemical formula	$RuC_{45}H_{38}N_2OClP_2$	$RuC_{51}H_{42}N_2OClP_2$
Formula weight	821.23	897.33
Crystal system	Orthorhombic	Triclinic
Space group	*Pbca*	$P\bar{1}$
Unit cell dimensions		
a (Å)	17.9809(9)	9.9424(5)
b (Å)	17.7702(9)	12.1929(6)
c (Å)	24.2867(12)	18.9142(9)
α (°)	90	94.610(1)
β (°)	90	104.140(1)
γ (°)	90	94.449(1)
V (Å^3)	7760.2(7)	2205.0(2)
Z	8	2
ρ (g cm^{-3})	1.406	1.352
μ (mm^{-1})	0.593	0.528
Reflections collected	45509	24430
Reflections unique	9295	9903
Reflections [$I \geqslant 2\sigma(I)$]	5190	7777
Parameters	470	524
R_1, wR_2 ($I \geqslant 2\sigma(I)$)	0.0623, 0.1003	0.0458, 0.0920
R_1, wR_2 (all data)	0.1301, 0.1190	0.0628, 0.0982
GOF on F^2	0.972	0.981
Largest peak and hole (e Å^{-3})	0.931 and −0.522	1.247 and −0.466

used for data extraction [18]. The data were corrected for absorption with the help of SADABS program [19]. Complexes **1** and **3** crystallize in the space groups *Pbca* and $P\bar{1}$, respectively. The structures were solved by direct methods and refined on F^2 by full-matrix least-squares procedures. In each case, the asymmetric unit contains one complete complex molecule. All non-hydrogen atoms were refined anisotropically. The hydrogen atoms were included in the structure factor calculation at idealized positions by using a riding model. The SHELX-97 programs [20] were used for structure solution and refinement. The ORTEX6a package [21] was used for molecular graphics. Selected crystallographic data are listed in Table 1.

3. Results and discussion

3.1. Synthesis and characterization

Reactions of $[Ru(PPh_3)_3Cl_2]$, the Schiff bases and $N(C_2H_5)_3$ (1:1:2 mole ratio) in methanol under aerobic conditions produce the complexes **1**–**6** in moderate yields. For **1**, boiling of the reaction mixture under reflux condition was necessary, while for **2**–**6** stirring at room temperature was sufficient. In the latter cases, boiling causes contamination of the products by colourless *mer*-$[Ru(CO)(H)_2(PPh_3)_3]$ [22,23]. We have confirmed the identity of this impurity by determining its X-ray structure which has been already published [22]. Formation of this carbonyl containing complex from $[Ru(PPh_3)_3Cl_2]$ in the presence of potassium aryloxide in methanol–dichloromethane mixture has been reported recently [23]. The elemental analysis data for the complexes are satisfactory with the general molecular formula $[Ru(L^n)(PPh_3)_2Cl]$ (Table 2). The complexes are highly soluble in dichloromethane and chloroform, affording yellow (**1**) to brown (**2**–**6**) solutions. However, except **1** the other complexes are not stable in solution. After about 1/2 h the colour changes to green. Despite our best efforts, we have not been able to isolate and characterize these green species. For this reason all the spectroscopic studies (*vide infra*) have been performed within 5 min after the preparation of the solutions. In solutions, all the complexes are electrically non-conducting. The room temperature (298 K) magnetic moments of **1**–**6** in powder phase are in the range 1.89–2.09 μ_B (Table 2). These values are consistent with the +3 oxidation state and low-spin character ($S = 1/2$ ground state) of the metal ions. It is very likely that the aerial oxygen acts as the oxidizing agent in the oxidation of the metal ion during the synthesis of these complexes from the ruthenium(II) starting material $[Ru(PPh_3)_3Cl_2]$.

3.2. Spectroscopic properties

The infrared spectra of **1**–**6** do not display the characteristic bands associated with the N–H and the C=O bonds of the amide functionality [24,25] present in the free Schiff bases. Thus the amide functionality is in the enolate form and the ligand coordinates the metal ion through the amide-O and the imine-N to form a five-membered ring as commonly observed in the complexes with Schiff bases derived from acid hydrazides [14,15,26–29]. A medium to strong band observed in the range 1564–1605 cm^{-1} is assigned to the conjugated —C=N—N=C— fragment of the ligand [14,15,26–29]. Three strong bands observed in the ranges 741–747, 693–696 and 515–521 cm^{-1} indicate the presence of ruthenium bound PPh_3. Similar bands are reported for complexes containing the *trans*-$\{Ru(PPh_3)_2\}$ unit [12,28–30].

The electronic spectroscopic data of **1**–**6** in dichloromethane solutions are listed in Table 2. The spectral profiles are quite similar. The moderately intense absorptions in the visible region are perhaps due to the ligand-to-metal charge transfer transitions [10–13,27,29,30]. The intense absorptions in the higher energy region are likely to be due to the ligand based transitions.

The EPR spectral profiles of **1**–**6** in frozen (120 K) dichloromethane–toluene (1:1) solutions are very similar. A representative spectrum is shown in Fig. 1. Each complex displays three distinct signals (Table 3) indicating the distortion of the $CNOClP_2$ coordination sphere around the metal centre from octahedral symmetry. This distortion can be divided into axial (Δ) and rhombic (V) components. The axial distortion splits the t_2 level into "a" and "e" and the rhombic component again splits "e" into non-degenerate components (Fig. 1). In addition to Δ and V, spin–orbit coupling also affects the extent of energy gaps between

Table 2
Elemental analysis, electronic spectroscopic[a] and magnetic susceptibility[b] data

Complex	Found (Calc.) (%)			λ_{max} (nm) ($10^{-4} \times \varepsilon$ (M^{-1} cm^{-1}))	μ_{eff} (μ_B)
	C	H	N		
1	65.72 (65.81)	4.58 (4.66)	3.34 (3.41)	450 (0.34), 380[c] (1.1), 353 (1.8), 270 (7.3)	2.06
2	67.75 (67.99)	4.49 (4.56)	3.05 (3.17)	495[c] (0.31), 410 (0.79), 308 (3.5), 260[c] (5.9)	2.05
3	68.13 (68.26)	4.61 (4.72)	3.10 (3.12)	482[c] (0.27), 407[c] (0.58), 323[c] (1.8), 245[c] (6.6)	1.92
4	66.89 (67.07)	4.50 (4.63)	2.98 (3.07)	480[c] (0.35), 415[c] (0.67), 315[c] (3.1), 247 (8.3)	2.09
5	65.26 (65.43)	4.14 (4.28)	2.87 (3.05)	490[c] (0.33), 418 (0.65), 310[c] (2.5), 245 (5.6)	1.94
6	64.41 (64.69)	4.05 (4.23)	4.32 (4.53)	505[c] (0.36), 445[c] (0.62), 350[c] (2.4), 250 (4.9)	1.89

[a] In dichloromethane.
[b] At 298 K.
[c] Shoulder.

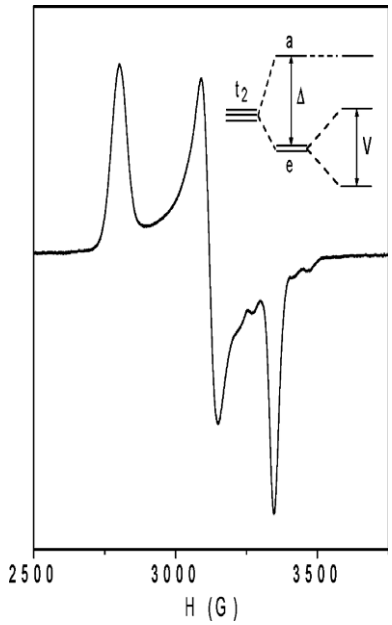

Fig. 1. X-band EPR spectrum of *trans*-[Ru(L^1)(PPh_3)$_2$Cl] (**1**) in dichloromethane–toluene (1:1) glass (120 K) and the t_2 splitting pattern.

these levels. Thus, two ligand-field transitions of energies ΔE_1 and ΔE_2 ($\Delta E_1 < \Delta E_2$) are possible within these three levels. The distortion parameters and the transition energies have been calculated using the EPR *g*-values and the g tensor theory for low-spin d^5 metal ion complexes [31]. The calculated values are listed in Table 3. In all the complexes, the axial and the rhombic distortions are comparable. The ΔE_1 transition is expected to occur in the range 4644–6359 cm^{-1} (2144–1573 nm), while the ΔE_2 transition is expected to occur within 13,535–18,146 cm^{-1} (739–551 nm) (Table 3). However, no absorption could be detected in the ΔE_1 region, perhaps due to the low intensity of this absorption [10–13,31] and the poor transparency of the solvent. No band could be observed in the ΔE_2 region also as it falls on the onset of the moderately intense absorption observed in the range 505–450 nm (Table 2).

3.3. X-ray structures of *1* and *3*

The molecular structures of **1** and **3** are depicted in Figs. 2 and 3, respectively. Selected bond parameters are listed in Table 4. In each molecule, the metal centre is in a distorted octahedral $CNOClP_2$ coordination sphere. The meridional tridentate ligand ((L^1)$^{2-}$ in **1** and (L^3)$^{2-}$ in **3**) coordinates the metal centre via the aromatic-C, the imine-N and the deprotonated amide-O atoms forming two five-membered chelate rings. The chloride completes a CNOCl square-plane (maximum deviation 0.05 Å for **1** and 0.04 Å for **3**) around the metal centre. As commonly observed for hexa-coordinated complexes containing the {Ru(PPh_3)$_2$} unit, the two bulky PPh_3 molecules occupy the remaining two axial sites [11,28–30]. The N(2)–C(8) and C(8)–O bond lengths are consistent with the enolate (—N=C(O^-)—) form of the amide functionality in the tridentate ligands [14,15,26–29]. The five-membered chelate rings are highly planar. In the chelate ring formed by Ru, N(1), N(2), C(8) and O, the maximum deviation is 0.03 Å for **1** and 0.01 Å for **3**. All deviations are below 0.02 Å for **1** and 0.006 Å for **3** in the chelate ring formed by Ru, C(1), C(6), C(7) and N(1). Both chelate ring planes are essentially

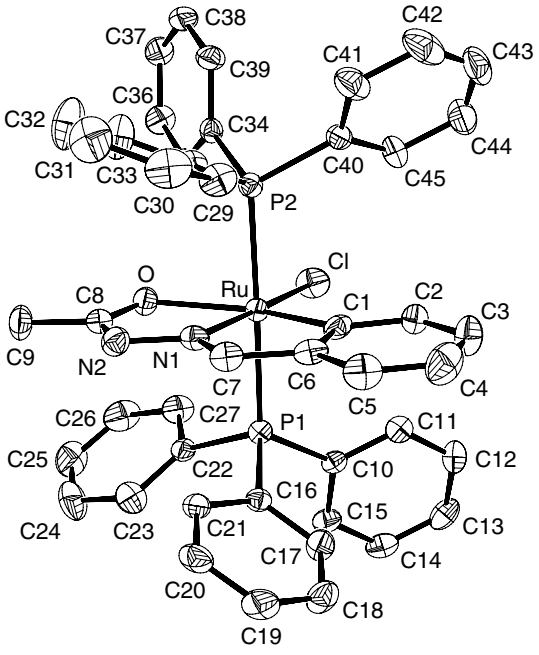

Fig. 2. Molecular structure of *trans*-[Ru(L^1)(PPh_3)$_2$Cl] (**1**) with the atom labeling scheme. All atoms are represented by their 30% probability thermal ellipsoids. Hydrogen atoms are omitted for clarity.

Table 3
EPR *g*-values,[a] distortion parameters and near-IR transitions[b]

Complex	g_1	g_2	g_3	Δ/λ	V/λ	$\Delta E_1/\lambda$	$\Delta E_2/\lambda$
1	2.34	2.10	1.96	12.169	−11.774	6.359	18.146
2	2.35	2.10	1.95	10.711	−10.239	5.768	15.931
3	2.32	2.07	1.93	8.984	−8.858	4.664	13.535
4	2.33	2.11	1.95	10.051	−8.622	5.822	14.469
5	2.35	2.11	1.95	10.381	−9.373	5.779	15.172
6	2.34	2.09	1.95	10.895	−10.771	5.598	16.380

[a] In 1:1 dichloromethane–toluene at 120 K.
[b] The calculations are based on the spin–orbit coupling constant (λ) = 1000 cm^{-1}.

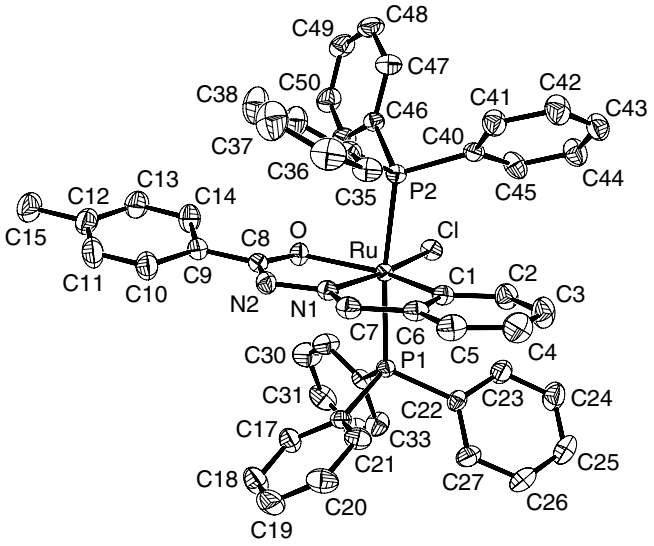

Fig. 3. Molecular structure of *trans*-[Ru(L^3)(PPh_3)$_2$Cl] (**3**) with the atom labeling scheme. All atoms are represented by their 30% probability thermal ellipsoids. Hydrogen atoms are omitted for clarity.

Table 4
Selected bond parameters for *trans*-[Ru(L^1)(PPh_3)$_2$Cl] (**1**) and *trans*-[Ru(L^3)(PPh_3)$_2$Cl] (**3**)

Complex	**1**	**3**
Bond lengths (Å)		
Ru–O	2.153(3)	2.1455(18)
Ru–Cl	2.3588(12)	2.3598(7)
Ru–N(1)	2.030(3)	2.028(2)
Ru–C(1)	2.041(4)	2.051(3)
Ru–P(1)	2.4050(11)	2.3992(7)
Ru–P(2)	2.3835(11)	2.3930(7)
N(2)–C(8)	1.326(5)	1.307(4)
C(8)–O	1.272(5)	1.288(3)
Bond angles (°)		
O–Ru–Cl	100.20(8)	96.57(5)
O–Ru–N(1)	74.16(12)	73.87(8)
O–Ru–C(1)	151.09(14)	150.85(10)
O–Ru–P(1)	91.66(8)	96.16(6)
O–Ru–P(2)	86.88(8)	90.26(6)
Cl–Ru–N(1)	173.92(10)	170.42(7)
Cl–Ru–C(1)	108.66(13)	112.41(8)
Cl–Ru–P(1)	89.40(4)	87.98(2)
Cl–Ru–P(2)	90.51(4)	88.40(2)
N(1)–Ru–C(1)	77.08(16)	77.17(10)
N(1)–Ru–P(1)	88.52(10)	92.41(7)
N(1)–Ru–P(2)	91.42(10)	92.17(7)
C(1)–Ru–P(1)	90.51(12)	88.26(8)
C(1)–Ru–P(2)	90.94(12)	87.53(8)
P(1)–Ru–P(2)	178.50(4)	172.95(3)

coplanar. The dihedral angle between the two chelate ring planes is 1.23(2)° and 3.69(8)° for **1** and **3**, respectively. The chelate bite angle formed by the imine-N and the amide-O (74.16(12)° for **1** and 73.87(8)° for **3**) is slightly smaller than that formed by the aromatic-C and the imine-N (77.08(16)° for **1** and 77.17(10)° for **3**). All other *cis* angles are in the ranges 86.88(8)–108.66(13)° and 87.53(8)–112.41(8)° for **1** and **3**, respectively. The P(1)–Ru–P(2) is the largest (178.50(4)° for **1** and 172.95(3)° for **3**), while O–Ru–C(1) is the smallest (151.09(14)° for **1** and 150.85(10)° for **3**) *trans* angle in both cases. The *trans* Cl–Ru–N(1) angle is 173.92(10) and 170.42(7)° for **1** and **3**, respectively. The bond lengths associated with the metal ion in **1** and **3** are very similar. The Ru–N(imine) and the Ru–O(amide) bond lengths are comparable with the bond lengths observed in ruthenium(III) complexes containing the same coordinating atoms [27,29]. The Ru–P bond lengths are similar to those reported for ruthenium(III) complexes containing the *trans*-{Ru(PPh_3)$_2$} moiety [11,29,30]. The Ru–Cl bond lengths in **1** and **3** are unexceptional [29,30]. All the complexes (**1**–**6**) have the general molecular formula [Ru(L^n)(PPh_3)$_2$Cl] and similar spectroscopic and electrochemical properties (*vide infra*). Hence, they are assumed to have similar molecular structures as observed for **1** and **3**.

3.4. Electron transfer properties

Electron transfer properties of **1**–**6** in dichloromethane solutions have been investigated by cyclic voltammetry. None of the complexes shows any response on the cathodic side of Ag/AgCl reference electrode. Complex **1** displays an irreversible oxidation at 0.98 V, while complexes **2**–**6** display a reversible oxidation in the potential range 0.35–0.58 V. In the latter cases, the peak-to-peak separations are within 80–90 mV and the cathodic and the anodic peak currents are essentially identical. A representative cyclic voltammogram is shown in Fig. 4 and the potential data are listed in Table 5. The one-electron stoichiometry of this oxidation response is confirmed by comparing the current heights with known one-electron redox processes under identical conditions [12,26–30,32]. The free ligands do not

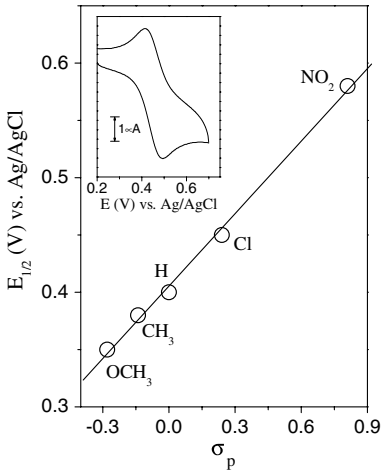

Fig. 4. Correlation between the $E_{1/2}$ values for the ruthenium(IV)–ruthenium(III) couple and the Hammett substituent constants. The straight line represents a linear least-squares fit. Inset: Cyclic voltammogram (scan rate 50 mV s^{-1}) of *trans*-[Ru(L^2)(PPh_3)$_2$Cl] (**2**) in dichloromethane solution (0.1 M TBAP).

Table 5
Cyclic voltammetric[a,b] data

Complex	$E_{1/2}$ (V)	ΔE_p (mV)
trans-[Ru(L^1)(PPh_3)$_2$Cl] (**1**)	0.98[c]	–
trans-[Ru(L^2)(PPh_3)$_2$Cl] (**2**)	0.40	80
trans-[Ru(L^3)(PPh_3)$_2$Cl] (**3**)	0.38	90
trans-[Ru(L^4)(PPh_3)$_2$Cl] (**4**)	0.35	80
trans-[Ru(L^5)(PPh_3)$_2$Cl] (**5**)	0.45	80
trans-[Ru(L^6)(PPh_3)$_2$Cl] (**6**)	0.58	90

[a] In dichloromethane solution (298 K) at a scan rate of 50 mV s^{-1}.
[b] $E_{1/2} = (E_{pa} + E_{pc})/2$, where E_{pa} and E_{pc} are anodic and cathodic peak potentials, respectively; $\Delta E_p = E_{pa} - E_{pc}$.
[c] E_{pa} value.

display any response in the above potential range. Thus the observed oxidation is assigned to ruthenium(III) to ruthenium(IV) process. It may be noted that the previously reported cyclometallated ruthenium(III) complexes of aromatic-C, azo- or imine-N and phenolate-O donor ligands also display similar ruthenium(III) to ruthenium(IV) oxidation responses [10–13]. In these complexes, the stability of the +3 oxidation state and the accessibility of the +4 state are primarily attributed to the phenolate-O coordination [10–13]. In the present series of complexes (**1**–**6**), a similar situation prevails due to the deprotonated amide-O coordination. The significantly higher potential for **1** compared to the potentials of **2**–**6** indicates easy accessibility of the +4 oxidation state of the metal centre due to aroyl amide-O coordination than acetyl amide-O coordination. The irreversible nature of the oxidation in the case of **1** suggests that the oxidized species is unstable in the cyclic voltammetry time scale. In the cases of **2**–**6**, the trend in the $E_{1/2}$ values of the ruthenium(IV)–ruthenium(III) couple reflects the effect of the electronic nature of the substituents (R) on the aroyl fragment of the tridentate ligands. For the most electron withdrawing substituent ($R = NO_2$) the oxidation of the metal ion occurs at the highest potential while for the most electron releasing substituent ($R = OCH_3$) it occurs at the lowest potential (Table 5). A satisfactory linear relationship is observed (Fig. 4) when the $E_{1/2}$ values are plotted against the Hammett substituent constants (σ_p) [33]. Thus, as the σ-bonding ability of the amide-O of the tridentate ligand decreases with the increasing electron withdrawing effect of the substituent, the ruthenium(III) to ruthenium(IV) oxidation becomes more difficult.

4. Conclusion

A new series of rare cyclometallated ruthenium(III) complexes having the general formula *trans*-[Ru(L)-(PPh_3)$_2$Cl] with Schiff bases (H_2L) prepared from acid hydrazides and benzaldehyde have been synthesized and characterized. In these complexes, the meridionally spanning bianionic tridentate ligand (L^{2-}) is C,N,O-donor to the metal centre. The molecular structures have been confirmed by X-ray structure determination of two representative complexes. These complexes provide very good examples of ruthenium mediated activation of *ortho*-C–H bond of the pendant phenyl group of H_2L. All the complexes are one-electron paramagnetic and display rhombic EPR spectra typical of ruthenium(III) complexes containing distorted octahedral low-spin metal centres. The complexes are redox active and display a metal centred oxidation. The potential of this ruthenium(IV)–ruthenium(III) couple is sensitive to the polar effect of the substituent on the aroyl moiety of the ligand.

5. Supplementary material

CCDC 620905 and 620906 contain the supplementary crystallographic data for *trans*-[Ru(L^1)(PPh_3)$_2$Cl] (**1**) and *trans*-[Ru(L^3)(PPh_3)$_2$Cl] (**3**), respectively. These data can be obtained free of charge via http://www.ccdc.cam.ac.uk/conts/retrieving.html, or from the Cambridge Crystallographic Data Centre, 12 Union Road, Cambridge CB2 1EZ, UK; fax: (+44) 1223-336-033; or e-mail: deposit@ccdc.cam.ac.uk.

Acknowledgements

Financial support for this work was provided by the Council of Scientific and Industrial Research, New Delhi (Grant No. 01(1880)/03/EMR-II). X-ray crystal structures were determined at the National Single Crystal Diffractometer Facility, School of Chemistry, University of Hyderabad (funded by the Department of Science and Technology, New Delhi). We thank the University Grants Commission, New Delhi for the facilities provided under the UPE and CAS programs.

References

[1] G. Wilkinson, F.G.A. Stone, E.W. Abel (Eds.), Comprehensive Organometallic Chemistry, vol. 4, Pergamon, Oxford, 1982, p. 651.
[2] D.F. Schriver, M.I. Bruce (Eds.), Comprehensive Organometallic Chemistry II, vol. 7, Pergamon, Oxford, 1995, p. 291.
[3] A.J. Hewitt, J.H. Holloway, R.D. Peacock, J.B. Raynor, I.L. Wilson, J. Chem. Soc., Dalton Trans. (1976) 579.
[4] L.H. Pignolet, S.H. Wheeler, Inorg. Chem. 19 (1980) 935.
[5] M.M. Taqui Khan, D. Srinivas, R.I. Kureshy, N.H. Khan, Inorg. Chem. 29 (1990) 2320.
[6] M. Ke, S.J. Rettig, B.R. James, D. Dolphin, J. Chem. Soc., Chem. Commun. (1987) 1110.
[7] J.W. Seyler, C.R. Leidner, Inorg. Chem. 29 (1990) 3636.
[8] M. Ke, C. Sishta, B.R. James, D. Dolphin, J.W. Sparapany, J.A. Ibers, Inorg. Chem. 30 (1991) 4766.
[9] M. Beley, J.-P. Collin, R. Louis, B. Metz, J.-P. Sauvage, J. Am. Chem. Soc. 113 (1991) 8521.
[10] G.K. Lahiri, S. Bhattacharya, M. Mukherjee, A.K. Mukherjee, A. Chakravorty, Inorg. Chem. 26 (1987) 3359.
[11] P. Ghosh, A. Pramanik, N. Bag, G.K. Lahiri, A. Chakravorty, J. Organomet. Chem. 454 (1993) 237.
[12] R. Hariram, B.K. Santra, G.K. Lahiri, J. Organomet. Chem. 540 (1997) 155.
[13] P. Munshi, R. Samanta, G.K. Lahiri, J. Organomet. Chem. 586 (1999) 176.
[14] S. Das, S. Pal, J. Organomet. Chem. 689 (2004) 352.
[15] S. Das, S. Pal, J. Organomet. Chem. 691 (2006) 2575.

[16] T.A. Stephenson, G. Wilkinson, J. Inorg. Nucl. Chem. 28 (1966) 945.
[17] W.E. Hatfield, in: E.A. Boudreaux, L.N. Mulay (Eds.), Theory and Applications of Molecular Paramagnetism, Wiley, New York, 1976, p. 491.
[18] SMART version 5.630 and SAINT-plus version 6.45, Bruker-Nonius Analytical X-ray Systems Inc., Madison, WI, USA, 2003.
[19] G.M. Sheldrick, SADABS, Empirical Absorption Correction Program, University of Göttingen, Göttingen, Germany, 1997.
[20] G.M. Sheldrick, SHELX-97, Structure Determination Software, University of Göttingen, Göttingen, Germany, 1997.
[21] P. McArdle, J. Appl. Crystallogr. 28 (1995) 65.
[22] P.C. Junk, J.W. Steed, J. Organomet. Chem. 587 (1999) 191.
[23] J.L. Snelgrove, J.C. Conrad, G.P.A. Yap, D.E. Fogg, Inorg. Chim. Acta 345 (2003) 268.
[24] W. Kemp, in: Organic Spectroscopy, Macmillan, Hampshire, 1987, pp. 62–65.
[25] K. Nakamoto, in: Infrared and Raman Spectra of Inorganic and Coordination Compounds, Wiley, New York, 1986, pp. 241–244.
[26] S.N. Pal, S. Pal, J. Chem. Soc., Dalton Trans. (2002) 2102.
[27] S.N. Pal, S. Pal, Eur. J. Inorg. Chem. (2003) 4244.
[28] R. Raveendran, S. Pal, Polyhedron 24 (2005) 57.
[29] R. Raveendran, S. Pal, Inorg. Chim. Acta 359 (2006) 3212.
[30] F. Basuli, A.K. Das, G. Mostafa, S.-M. Peng, S. Bhattacharya, Polyhedron 19 (2000) 1663.
[31] S. Bhattacharya, A. Chakravorty, Proc. Indian Acad. Sci. (Chem. Sci.) 95 (1985) 159.
[32] S.G. Sreerama, S. Pal, Inorg. Chem. 44 (2005) 6299.
[33] J. March, in: Advanced Organic Chemistry, 4th ed., Wiley, New York, 1992, p. 280.